

Chandra X-Ray Spectral Analysis of Cooling Flow Clusters, 2A 0335+096 and Abell 2199

Naomi KAWANO, Akimitsu OHTO, and Yasushi FUKAZAWA

Department of Physical Sciences, School of Science, Hiroshima University,

1-3-1 Kagamiyama, Higashi-Hiroshima, Hiroshima 739-8526

kawano@hirax7.hepl.hiroshima-u.ac.jp

(Received 2002 August 27; accepted 2003 March 24)

Abstract

We report on a spatially resolved analysis of Chandra X-ray data on a nearby typical cooling flow cluster of galaxies 2A 0335+096, together with A 2199 for a comparison. As recently found in the cores of other clusters, the temperature around the central part of 2A 0335+096 is 1.3–1.5 keV, which is higher than that inferred from the cooling flow picture. Furthermore, the absorption column density is almost constant against the radius in 2A 0335+096; there is no evidence of excess absorption up to 200–250 kpc. This indicates that no significant amount of cold material, which has cooled down, is present. These properties are similar to those of A 2199. Since the cooling time in the central part is much shorter than the age of the clusters, a heating mechanism, which weakens the effect of radiative cooling, is expected to be present in the central part of both clusters of galaxies. Both 2A 0335+096 and A 2199 have radio jets associated with their cD galaxy. We discuss the possibility of heating processes caused by these radio jets by considering the thermal conduction and the sound velocity together with the observed disturbance of the ICM temperature and density. We conclude that the observed radio jets can produce local heating and/or cooling, but do not sufficiently reduce the overall radiative cooling. This implies that much more violent jets, whose emission has now decayed, heated up the cooling gas $> 10^9$ years ago.

Key words: galaxies: clusters: individual (2A 0335+096, Abell 2199) — galaxies: cooling flows — galaxies: intergalactic medium — X-rays: galaxies

1. Introduction

Many clusters of galaxies exhibit a sharp profile around the X-ray emission peak at the center, and their intracluster medium (ICM) becomes cooler toward their center. This is apparently consistent with the idea of a cooling flow model (review; Fabian 1994). However, other observational phenomena have also been found and cannot agree with the simple cooling flow picture (Makishima et al. 2001; Tamura et al. 2001a). In order to obtain more information about the physical condition of the ICM in the central part of clusters, spatially resolved measurements of the temperature, absorption column density, and metal abundance are needed. The spatial resolution and effective area of previous X-ray satellites did not allow us to resolve the innermost cluster regions in detail.

Recent observations with Chandra and XMM-Newton revealed complex physical properties of the ICM in the central region of the Perseus cluster (Fabian et al. 2000; Schmidt et al. 2002), Hydra-A cluster (McNamara et al. 2000; David et al. 2001), A 1795 (Tamura et al. 2001a; Fabian et al. 2001; Ettori et al. 2002), A 1835 (Schmidt et al. 2001; Peterson et al. 2001), and A 496 (Tamura et al. 2001b) clusters, which are typical cooling flow clusters. One of the important results is that the ICM temperature at the central region is not as low as ~ 1 keV, which is expected from the simple cooling flow model. X-ray emission of the Perseus and Hydra-A clusters shows holes with X-ray bright rims, which are caused by an ICM displacement by the radio jet. These results indicate that the radio jet is violently interacting with the ICM, and is thus a possible candidate of heating sources which would reduce the cooling flow. However, the ICM temperature of bright rims surrounding the radio jet in the Perseus cluster is ~ 2.7 keV, which is cooler than the ambient ICM. In the case of the Hydra-A cluster, there is no correlation between the radio jets and spectral hardening due to shock of radio jet. On the other hand, evidence of jet heating is reported for MKW3s (Mazzotta et al. 2002). The region of depression in the X-ray surface brightness, which lies south of the X-ray peak, exhibits a higher temperature than the surrounding one, indicating energy injection from the central radio galaxy.

In this way, two contrasting results coexist concerning whether the heating mechanism associated with radio jets exists or not. Therefore, it is important to obtain much more information on the X-ray properties in the central cluster region. 2A 0335+096 ($z = 0.035$) and A 2199 ($z = 0.0305$) are nearby X-ray bright cooling flow clusters of galaxies. The cooling flow rates are relatively large, $181 M_{\odot} \text{ yr}^{-1}$ (Edge et al. 1992) and $90 M_{\odot} \text{ yr}^{-1}$ (Owen, Eilek 1998), for 2A 0335+096 and A 2199, respectively. They are accompanied by radio jets at their center, especially for A 2199, whose radio jets from the cD galaxy NGC 6166 seem to interact with the ICM (Owen, Eilek 1998). It is thus possible that heating or cooling by the radio jets takes place in the central region of both clusters. According to these properties, they are good targets to approach the problems on the cooling flow, in terms of the temperature structure and excess

absorption. They are bright enough to be resolved finely by the Chandra observatory with good photon statistics. The spectral coverage provided by Chandra allows an accurate estimate of their ICM temperature, which is expected to be around 4 keV. Significant excess absorption was reported for 2A 0335+096 by White et al. (1991) based on the Einstein SSS observation; they claimed that it is attributed to cooling flow. The low galactic absorption toward A 2199 is also advantageous to constrain excess absorption. The high spatial resolution provided by Chandra allows us to spatially resolve the X-ray emission of these clusters on the arcseconds scale.

We report in this paper on spatial and spectral analyses of 2A 0335+096 and A 2199, both observed with ACIS-S on board Chandra. The results of an analysis of the Chandra observation of A 2199 was presented by Johnstone et al. (2002), who derived several X-ray properties of the central cooling region. Since these two clusters are a good pair for a comparison to understand the central cooling region of clusters of galaxies, as described above, we also reanalyzed the Chandra data on A 2199 in the same way as for 2A 0335+096. Throughout this paper, we assume $H_0 = 50 \text{ km s}^{-1} \text{ Mpc}^{-1}$; $1'' = 1.02 \text{ kpc}$ for 2A 0335+096 and $1'' = 0.89 \text{ kpc}$ for A 2199, respectively.

2. Observation

We observed 2A 0335+096 on 2000 September 16, with a back-illuminated CCD chip, ACIS-S3, loaded onto Chandra. The total exposure time was 20 ks (obsid 919). A 2199 was also observed with the Chandra ACIS-S3 on 1999 December 11. For A 2199, we used archival data (obsid 498), and the total exposure time was 19 ks. When we started the analysis, no blank sky data were available, and thus we employed data of the galaxy NGC 3184 as background, since it was observed in the same ACIS set up as both clusters, and does not contain any bright X-ray sources. We confirmed that the background level of the NGC 3184 data is consistent with that of on-source data. The background was estimated in the same detector region as on-source data by using the software *acisbg* which is provided by Maxim Markevitch¹. All of the data retrieved from the Chandra Data Center were at level 1–2. We used the CIAO 2.0 software package provided by CXC for the data analysis, and all spectra were corrected with the calibration product CALDB 2.9.

3. Analysis and Results

3.1. X-Ray Imaging Analysis of 2A 0335+096

The X-ray image of 2A 0335+096 in the 0.4–9.0 keV band is shown in figure 1a. The X-ray emission of 2A 0335+096 does not seem to be circularly symmetric; the south region of the center is brighter and the NE region is relatively fainter. A hole is seen in the direction

¹ <http://hea-www.harvard.edu/maxim/axaf/acisbg/>

of NW at $40''$ of the cluster center. This hole is not associated with any radio sources, and is thus thought to be the same feature as ‘ghost’ cavities reported for the Perseus cluster and Abell 2597 (Churazov et al. 2000; McNamara et al. 2001), which are considered to be fossils of radio-bright cavities after electron cooling. The VLA radio observation of 2A 0335+096, performed in 1987 and 1992, revealed that it has twin jets which emanate from the cD galaxy, and are extended up to $\sim 10''$ toward the NE and SW (Sarazin et al. 1995). The radio image in the central region of 2A 0335+096 is shown in figure 1b. A spatial resolution of $16''$ did not allow us to resolve finer structures comparable to the ones observed in Chandra. For the first time, however, we noticed a weak correlation between the X-ray emission and the radio jet in the direction of NE from the center, thanks to the high spatial resolution of Chandra. On the other hand, Johnstone et al. (2002) found that the X-ray emission of A 2199 is displaced by the radio jet at the center more clearly than 2A 0335+096. A short radio jet extending up to ~ 3 kpc is visible on the E and W sides of the cD galaxy.

In order to derive physical quantities of the ICM, such as the gas density, the X-ray surface brightness profile was fitted by the canonical β -model (Jones, Forman 1984), and is shown in figure 2. Here, the cluster center was determined to be the position of the cD galaxy, which almost coincides with the root of radio jets. The best-fit parameters and reduced chi-square are listed in table 1. The profile is rather well-fitted by a single β model; there is no excess in the X-ray surface brightness at the center. The β and core radius, r_c , are consistent with $\beta = 0.55$ of the ROSAT HRI observation (Sarazin et al. 1992) and $\beta = 0.60 \pm 0.05$ and $45'' \pm 15''$ of the ASCA GIS (Fukazawa 1997). Therefore, the X-ray surface brightness of 2A 0335+096 can be quite well represented by a single β -model from the most inner to outer region.

3.2. Radial Profiles of the Spectral Properties for 2A 0335+096

Although the ICM distribution of 2A 0335+096 is not circularly symmetric, as described in subsection 3.1, we first investigated the spectral variation toward the radial direction in order to understand the overall features of the ICM. To obtain radial profiles of the temperature, column density and metal abundance, spectral fittings were performed for several annuli centered on cD galaxies in the 0.5–10 keV region. The background spectra and response matrices were extracted from the corresponding region. The background-subtracted spectra are shown in figure 3a. Here, we pick up four characteristic spectra at $0'' - 10''$, $30'' - 40''$, $60'' - 90''$, and $150'' - 180''$ annuli. Fe-L lines become stronger and shift to the lower energy side as the radius becomes small, indicating that the temperature decreases toward the cluster center. We also show the spectra of A 2199 for comparison in figure 3b. It can be clearly seen that the absorption in the lower energy band is quite different between two clusters. This is mainly due to a large difference in the galactic column density: 1.7×10^{21} cm² and 8.7×10^{19} cm² for 2A 0335+096 and A 2199, respectively. This well demonstrates that the ACIS-S spectrum is very sensitive to the photoelectric absorption.

These spectra of 2A 0335+096 were fitted with a one-temperature MEKAL thermal-plasma model (Liedahl et al. 1995) with photoelectric absorption. The free parameters are the temperature (kT), column density (N_{H}), metal abundance (A_{Fe}) and normalization. As a result, the reduced chi-squares, χ^2/dof , are 1.1–1.6 for radii beyond $40''$, and 1.6–2.7 within $40''$. We then tried to fit the spectra with the two-temperature MEKAL model. The abundance is tied to be the same among two components, and the temperature of the hot component is fixed at 3.3 keV, which is that of the outermost region. The fittings were improved for spectra within $40''$ from the center, and the reduced chi-squares χ^2/dof became smaller by 0.3–0.5. The χ^2/dof of one and two-temperature fittings in the center of 2A 0335+096 are shown in table 2. The temperature of the cool component was 1.3–1.6 keV, somewhat lower by 0.2–0.3 keV than that in the fitting with the single-temperature model. Since the core radius of the X-ray surface brightness is about $35''$, the spectra within $40''$ are thought to be affected by a projection effect. However, the purpose of our work is to search for evidences of jet heating from relative temperature variations. The projection effect on the best-fit temperature is at most 0.2–0.3 keV, which is not very significant for our purpose. Therefore, here after, we discuss our results on the single-temperature model fitting. Figure 4 shows radial profiles of kT and N_{H} obtained from spectral fittings with the single-temperature MEKAL model.

We first refer to the temperature profile (figure 4a). At $150''$ from the cluster center, the temperature reaches ~ 3.3 keV, which is somewhat higher than the outer-region temperature obtained with ASCA: 3.0 ± 0.1 keV at $3' - 8'$ radius (Fukazawa et al. 1998). This might be an indication of a radial temperature decrease toward the outer region, as claimed by Markevitch et al. (1998). Moreover, the temperature declines toward the cluster center, as reported based on a ROSAT analysis (Irwin, Sarazin 1995). Our Chandra results present finer and clearer profiles. In the simple cooling flow model, the temperature is predicted to decline steeply down to < 1 keV at the center. However, the actual temperature profile does not indicate such a steep decline; the gas temperature within $30''$ is almost constant at ~ 1.5 keV. The temperature of the cool component in the two-temperature model is also higher than 1 keV. In the case of A 2199, the temperature at the center is reported to be ~ 2.0 keV, which is fairly high for the simple cooling flow picture. Interestingly, both clusters exhibit apparent differences of the temperature profiles. The low-temperature region in 2A 0335+096 is extended up to ~ 150 kpc ($\sim 150''$), while that of A 2199 is up to only ~ 100 kpc. The temperature profile in the very central region within $30''$ is flatter for 2A 0335+096 than for A 2199.

Secondly, regarding the absorption profiles (figure 4b), in the central region, the absorption is $\sim 2.8 \times 10^{21} \text{ cm}^{-2}$, which is consistent with the previous results of Einstein SSS (White et al. 1991), ROSAT PSPC (Irwin, Sarazin 1995), and ASCA (Kikuchi et al. 1999). Therefore, problems concerning the response matrix of ACIS-S in the lower energy band (Plucinsky et al. 2002) are not significant for our results. On the other hand, our results show that the absorption is almost constant up to $3'$ (~ 200 kpc). This indicates that there is no central

excess absorption, and therefore no evidence of a large amount of cool gas predicted from the cooling flow picture. From a 21 cm line observation (Stark et al. 1992), the hydrogen column density is estimated to be $\sim 1.71 \times 10^{21} \text{ cm}^{-2}$, which is half of the value compared with that inferred from the X-ray absorption. This discrepancy implies the possible existence of galactic interstellar gas with high metallicity toward the direction of 2A 0335+096.

Finally, we refer to the metal abundance. The metal abundance is almost constant around 0.3 solar with a small variation of ~ 0.1 solar over the ACIS-S field of view. This trend is consistent with the ASCA results of 0.34 ± 0.04 solar and 0.30 ± 0.03 solar (Fukazawa et al. 2000), which were derived from spectral fittings for the inner $2'$ and outer $3' - 8'$, respectively. A more detailed investigation on the metal abundance is beyond the scope of this paper. In summary, we have obtained results on the spectral properties of 2A 0335+096 that are consistent with the previous ones in the outskirts of the cluster, and definitely more accurate than previously published in the central regions, where we have spatially resolved the temperature and absorption distribution.

3.3. Temperature Map

In subsection 3.2, we mentioned that the central temperature is higher than that predicted from the cooling flow picture. This temperature profile can be explained if there is a certain heating mechanism against cooling, for example, radio jets or merging. Here, we consider any evidence of jet heating. To examine the relation between the azimuthal temperature variation and radio jets, we obtained temperature maps with $5''$ square grids in a $60'' \times 60''$ region around the cluster center. The background spectra and responses were prepared as described in the previous section. The single-temperature MEKAL plasma model was used again, and could fit the spectra well. We also performed this analysis on A 2199, since the square region of the temperature map obtained by Johnstone et al. (2002) is somewhat large for the scale of radio jets, and we would like to compare the maps with the same and finer grid scales.

Figure 5 shows two-dimensional temperature maps. The typical error of the temperature in each grid are 10% and 15% for 2A 0335+096 and A 2199, respectively. Both clusters exhibit an asymmetric temperature structure. In 2A 0335+096, although the radial temperature profile exhibits a gradual decrease toward the cluster center, as shown in figure 4a, the temperature structure around the central $60'' \times 60''$ region is fairly complex; there is no clear trend of circular symmetry. There are two hot regions of $5'' - 10''$ size along the jet direction (NE and SW), located at $15''$ from the center, where the temperature is somewhat higher by 0.3–0.5 keV than that in the surrounding region. A significant cool region is largely extended toward the SE region, and another local cool region exists at the NW direction. Both cool regions are located perpendicular to the jets, and their temperature is ~ 1.3 keV, lower than the central temperature of ~ 1.6 keV. We have found no evidence of a spectral hard component from jets or AGN. For A 2199, the overall temperature structure is consistent with that of Johnstone et

al. (2002), and the circular symmetry is relatively better than that of 2A 0335+096. The most noticeable cool region exists at the southern region of the center, and there is a weak hint of a higher temperature along the E and W jet directions.

In order to visualize the temperature variation more clearly and show the significance with error bars, we obtained the azimuthal temperature profiles with an azimuthal angle interval of $22^\circ.5$. The azimuthal temperature profiles were investigated on four concentric circles. At each azimuthal angle, the spectrum was integrated within a circle whose radius was chosen to be $5''$, $5''$, $10''$, or $15''$ on each concentric circle of $10''$, $20''$, $40''$ or $70''$ from the cluster center, respectively. The obtained azimuthal temperature profiles are shown in figure 6. Here, the azimuthal angle is defined as 0° for the northern direction from the cluster center, and increases clockwise. In 2A 0335+096, the central radio jets lie at 135° (NE: northeast) and 315° (SW: southwest). It is clearly seen that the azimuthal temperature profile exhibits a large variation, which has been already noted by figure 5a. The high-temperature region is seen at 320° for the inner region, which is almost the same direction as the SW jet. On the other hand, temperature depression exists around $200^\circ - 260^\circ$ at the outer region, which is perpendicular to jets. In A 2199, the radio jets lie at 90° (E: east) and 270° (W:west). A faint temperature depression is scarcely seen in the outer region around the E and W jets, as hinted in figure 5b.

As a result, some correlations between the temperature variation and radio jets are detected for both clusters, and 2A0335+096 exhibits a larger amplitude of the temperature variation. Therefore, we compared the radial temperature distributions between the jet direction and its perpendicular one, so that we can trace the region size of the temperature disturbance. The resulting temperature distributions are shown in figure 7. It can be seen that the profile is asymmetric. The NE jet (open circles in the left region of figure 7) shows a remarkably higher temperature at $10'' - 30''$ from the center than the opposite (SW), consistent with figure 6a. The SE temperature-depression region in figure 6a (around $200^\circ - 240^\circ$) is also clearly noticed at $20'' - 50''$ from the center in the left region of figure 7 (filled squares).

In summary, regions of both high and low temperature are found at $10'' - 40''$ from the center along the NE jet and the SE region for 2A 0335+096, while A 2199 exhibits an asymmetric temperature distribution in the direction perpendicular to the jets within $30''$ of the center, and has a low-temperature region at the end of the E and W jet.

4. Discussion

We analyzed Chandra data for 2A 0335+096 and A 2199 to obtain the spatially resolved central properties of the ICM. The X-ray surface brightness is not circularly symmetric at the center of both clusters. In 2A 0335+096, the SE part is brighter and a radio-quiet X-ray hole exists at the NW part, although we find no significant disturbance by radio jets. On the other hand, a clear correlation with the East–West radio jets is seen in A 2199; an X-ray emitting hot plasma is displaced by jets. The temperatures of both clusters gradually decrease toward

the center. However, the central temperatures of both clusters are not as low as < 1 keV; 1.6 keV and 2.0 keV for 2A 0335+096 and A 2199, respectively. An asymmetric temperature distribution is found around the radio jets and the central ~ 30 kpc region perpendicular to the jets. It is interesting that the temperature variation is milder for A 2199, which exhibits a clearer disturbance of the ICM density by jets. The radial profile of the absorption column density is fairly uniform, except for the central region within 50 kpc where some increases of $\sim 10^{20}$ cm $^{-2}$ are barely seen.

The cooling time at the radius where temperature starts to drop is 2×10^{10} yr at $160''$ (163 kpc) for 2A 0335+096 and $\sim 9 \times 10^9$ yr at $100''$ (89 kpc) for A 2199, based on our Chandra results and Johnstone et al. (2002). Therefore, it can be said that the low-temperature region exists within the cooling radius, which is defined as the radius where the cooling time is comparable to the age of the cluster ($\sim 10^{10}$ yr). This result seems to be consistent with the cooling flow picture. However, in this scenario, the action of radiative cooling leaves the central ICM to temperatures below 1 keV, values that we did not observe in the clusters under examination. In particular, a high temperature of ~ 2 keV at the center of A 2199 is not easy to explain. Therefore, the Chandra results for both clusters are not consistent with the simple cooling flow picture. Our results indicate that although radiative cooling may occur, some heating mechanisms would prevent the ICM from cooling down to $kT < 1$ keV.

An excess of the absorption column density toward the center of cooling-flow clusters is expected if a large amount of gas cools down and deposits at the cluster center. In the past, observations with the Einstein SSS reported the existence of absorbing cold matter (White et al. 1991), whose column density is $(5-10) \times 10^{20}$ cm $^{-2}$; also, ROSAT observations sometimes claimed an increase in the absorption column density toward the cluster center (e.g. Allen, Fabian 1997). Einstein SSS observations reported that 2A 0335+096 exhibits a significant excess of the absorption column density: 3.0×10^{21} cm $^{-2}$ against the galactic value of 1.7×10^{21} cm $^{-2}$. ROSAT PSPC observations also confirmed this value at the center of 2A 0335+096, and gave a hint of a gradual decrease of the absorption toward the outer region (Irwin, Sarazin 1995). However, the narrower energy band and poorer energy resolution of Einstein and ROSAT compared with the Chandra observatory did not allow us to constrain the absorption column density accurately, because of the complex spectral properties at the cluster center. Chandra ACIS-S, for the first time, determined the absorption column density accurately, as well as the radial distribution of the absorption, thanks to its energy resolution, wide energy band down to 0.3 keV, and superior angular resolution. As a result, there is no sign of significant excess in absorption for both clusters. A little evidence of excess absorption of $\sim 1 \times 10^{20}$ cm $^{-2}$ within 50 kpc of the center in both clusters can be explained by the cold interstellar medium of mass $\sim 10^9 M_{\odot}$ in the central galaxy. For 2A 0335+096, the absorption value, itself, at the cluster center is consistent with the previously observed results, and the radial decrease that was previously suggested was not observed by ACIS-S within ~ 200 kpc of the

center. Even if the distribution of cold material extends over ~ 200 kpc, the absorption must be the largest toward the cluster center. Therefore, our results rule out the existence of a large amount of cold material. It can be said that the ROSAT PSPC results are consistent with no absorption gradient, considering their large errors (Irwin, Sarazin 1995). However, a significant discrepancy remains that the obtained absorption is larger than the galactic value determined from radio observations. We suggest that unidentified molecular clouds in our Galaxy exist toward the direction of 2A 0335+096.

We obtained a fine temperature map around the cluster center, and found that the temperature varies locally and mildly. Both hot and cool regions are found along the radio jets, indicating that radio jets can certainly heat up the ICM locally and at the same time compress it to be adiabatically cooled. Considering these results, it is suggested that radio jets recently ejected from cD galaxies were not powerful enough to give a large amount of shock-heated energy to the ambient ICM. The temperature varies by about 1 keV on a scale of few tens of kpc at most with a gas density of 10^{-2} cm^{-3} , corresponding to work of $\sim 10^{57}$ erg. The cooling loss by radiation is estimated to be 10^{44} erg s^{-1} at the center of both clusters. We consider the effect of heat conduction, combined with the sound speed in the plasma, which reduces the temperature and density variation in the ICM. The heat conduction flux was calculated to be $\sim 10^{42}$ erg s^{-1} for an ~ 1 keV gradient in ~ 10 kpc (Spitzer 1956). This heat flux shows that the typical heated-up regions found in both clusters vanish within $\sim 10^7$ yr. The crossing time scale of the sound velocity is also of the same order. Hence, the ICM disturbance caused by jets can survive for as long as $\sim 10^7$ yr. The cumulative heating energy to reduce the radiative cooling over the past 10^7 yr should have been 10^{59} erg, which is about 100-times larger than that inferred from the present ICM disturbance; in other words, the relatively mild variation of the ICM temperature and the density in both clusters implies that jet heating in both clusters is not effective enough to restrain the cooling flow, at least during the last 10^{7-8} years. Therefore, cD galaxies should have ejected relativistic plasma and produced jets that are more powerful than that actually observed $> 10^7$ years ago by an order of magnitude, if radio jets are attributed to a reduction of the radiative cooling, setting aside other heating processes, such as merging. A few nearby clusters have such a powerful radio jet at a redshift of $z < 0.1$, like, e.g., the Cygnus-A cluster. This implies that most cD galaxies might have ejected quite a powerful radio jet in the past, and such an active phase might have ended 10^9 years ago.

The authors thank an anonymous referee for a careful reading of the text and many helpful comments. The authors are also grateful to the Chandra team for their help in the spacecraft operation, calibration, and data analysis.

References

Allen, S. W., & Fabian, A. C. 1997, MNRAS, 286, 583

Churazov, E., Forman, W., Jones, C., & Böhringer, H. 2000, *A&A*, 356, 788

David, L. P., Nulsen, P. E. J., McNamara, B. R., Forman, W., Jones, C., Ponman, T., Robertson, B., & Wise, M. 2001, *ApJ*, 557, 546

Edge, A. C., Stewart, G. C., & Fabian, A. C. 1992, *MNRAS*, 258, 177

Ettori, S., Fabian, A. C., Allen, S. W., & Johnstone, R. M. 2002, *MNRAS*, 331, 635

Fabian, A. C. 1994, *ARA&A*, 32, 277

Fabian, A. C., et al. 2000, *MNRAS*, 318L, 65

Fabian, A. C., Sanders, J. S., Ettori, S., Taylor, G. B., Allen, S. W., Crawford, C. S., Iwasawa, K., & Johnstone, R. M., 2001, *MNRAS*, 321L, 33

Fukazawa, Y. 1997, Ph.D. Thesis, The University of Tokyo

Fukazawa, Y., Makishima, K., Tamura, T., Ezawa, H., Xu, H., Ikebe, Y., Kikuchi, K., & Ohashi, T. 1998, *PASJ*, 50, 187

Fukazawa, Y., Makishima, K., Tamura, T., Nakazawa, K., Ezawa, H., Ikebe, Y., Kikuchi, K., & Ohashi, T. 2000, *MNRAS*313, 21

Irwin, J. A., & Sarazin, C. L. 1995, *ApJ*, 455, 497

Johnstone, R. M., Allen, S. W., Fabian, A. C., & Sanders, J. S. 2002, *MNRAS*, 336, 299

Jones, C. & Forman, W. 1984, *ApJ*, 276, 38

Kikuchi, K., Furusho, T., Ezawa, H., Yamasaki, N. Y., Ohashi, T., Fukazawa, Y., & Ikebe, Y. 1999, *PASJ*, 51, 301

Liedahl, D. A., Osterheld, A. L., & Goldstein, W. H. 1995, *ApJ*, 438L, 115

Markevitch, M., Forman, W. R., Sarazin, C. L., & Vikhlinin, A. 1998, *ApJ*, 503, 77

Makishima, K., et al. 2001, *PASJ*, 53, 401

Mazzotta, P., Kaastra, J. S., Paerels, F. B., Ferrigno, C., Colafrancesco, S., Mewe, R., & Forman, W. R. 2002, *ApJ*, 567, 37

McNamara, B. R., et al. 2000, *ApJ*, 534L, 135

McNamara, B. R., et al. 2001, *ApJ*, 562L, 149

Owen, F. N., & Eilek, J. A. 1998, *ApJ*, 493, 73

Peterson, J. R., et al. 2001, *A&A*, 365, 104

Plucinsky, P. P., et al. 2002, *astro-ph/0209161*

Sarazin, C. L., Baum, S. A., & O’Dea, C. P. 1995, *ApJ*, 451, 125

Sarazin, C. L., O’Connell, R. W., & McNamara, B. R. 1992, *ApJ*, 397L, 31

Schmidt, R. W., Allen, S. W., & Fabian, A. C. 2001, *MNRAS*, 327, 1057

Schmidt, R. W., Fabian, A. C., & Sanders, J. S. 2002, *MNRAS*, 337, 71

Spitzer, L. Jr. 1956, *Physics of Fully Ionized Gases* (New York: Interscience)

Stark, A. A., Gammie, C. F., Wilson, R. W., Bally, J., Linke, R. A., Heiles, C., & Hurwitz, M. 1992, *ApJS*, 79, 77

Tamura, T., et al. 2001a, *A&A*, 365L, 87

Tamura, T., Bleeker, J. A. M., Kaastra, J. S., Ferrigno, C., & Molendi, S. 2001b, *A&A*, 379, 107

White, D. A., Fabian, A. C., Johnstone, R. M., Mushotzky, R. F., & Arnaud, K. A. 1991, *MNRAS*, 252, 72

Table 1. Best-fit parameters from X-ray surface brightness fittings with the single β -model.

	β	r_c (arcsec)	Normalization (10^{-3} count s $^{-1}$ arcsec $^{-2}$)	χ^2
2A 0335+096	0.58	32.1	1.26	1.87

Table 2. χ^2/dof for the one (1T) and two (2T) temperature models.

Radius	χ^2/dof for 1T	χ^2/dof for 2T
0'' – 10''	201.9/129 (1.56)	155.3/128 (1.21)
10'' – 20''	498.1/187 (2.66)	385.0/186 (2.07)
20'' – 30''	492.4/210 (2.34)	346.7/209 (1.66)
30'' – 40''	412.2/221 (1.86)	357.7/220 (1.63)
40'' – 50''	347.2/229 (1.52)	310.0/228 (1.36)
50'' – 60''	325.7/228 (1.43)	297.4/227 (1.31)

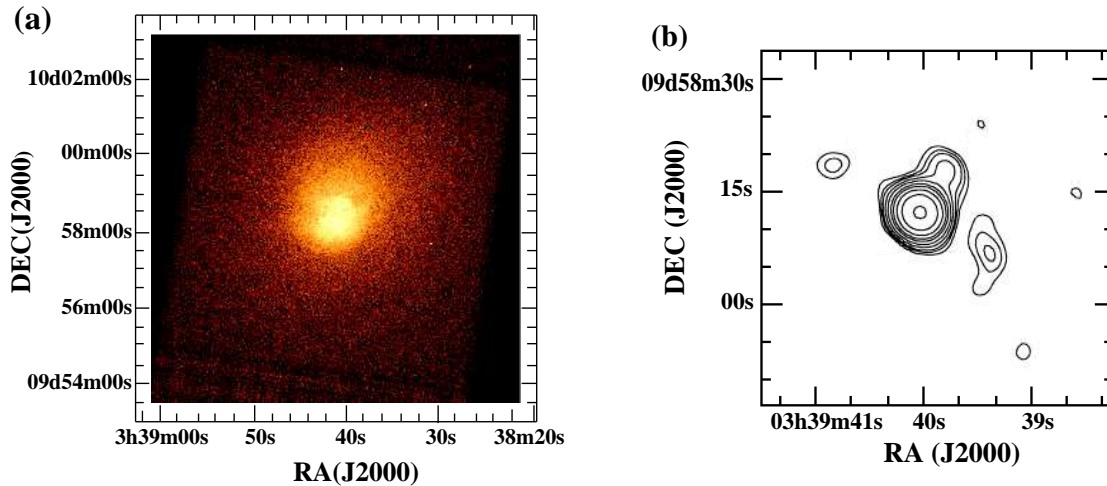


Fig. 1. Chandra ACIS-S3 X-ray image in the 0.4–9.0 keV band of 2A 0335+096 (a), and 8.4 GHz radio image in the central $50'' \times 50''$ region (b), which is quoted from Sarazin et al. (1995).

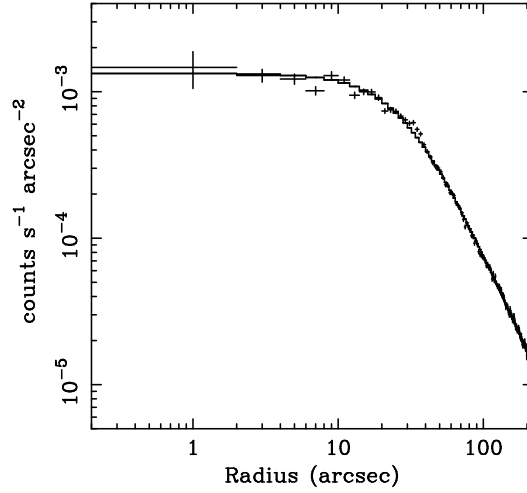


Fig. 2. X-ray surface brightness profile fitted with the β -model for 2A 0335+096.

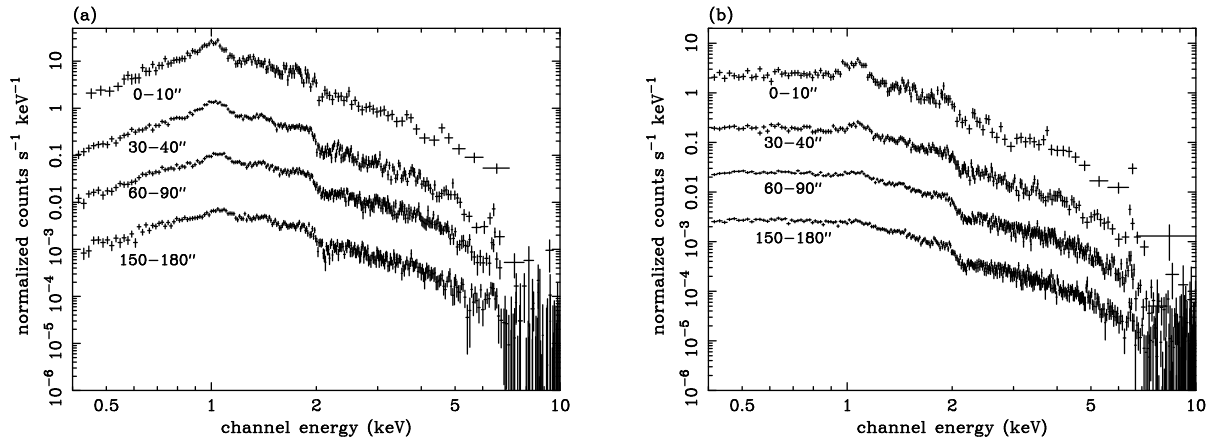


Fig. 3. Chandra ACIS X-ray spectra at four radii of $0'' - 20''$, $60'' - 80''$, $120'' - 180''$ and $300'' - 360''$ centered on the cluster center. (a) 2A 0335+096 and (b) A 2199.

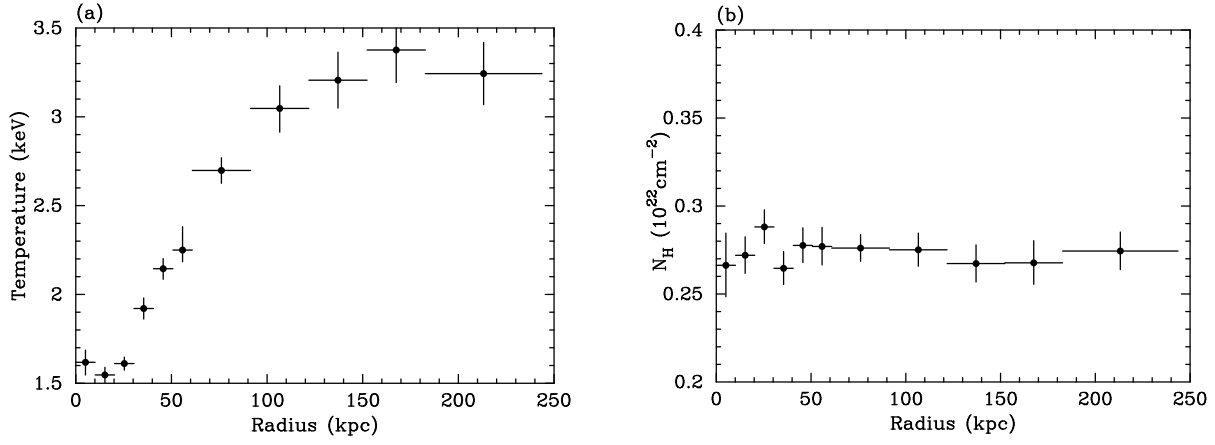


Fig. 4. Radial profiles of (a) the temperature, kT , and (b) the absorption column density, N_{H} , for 2A 0335+096.

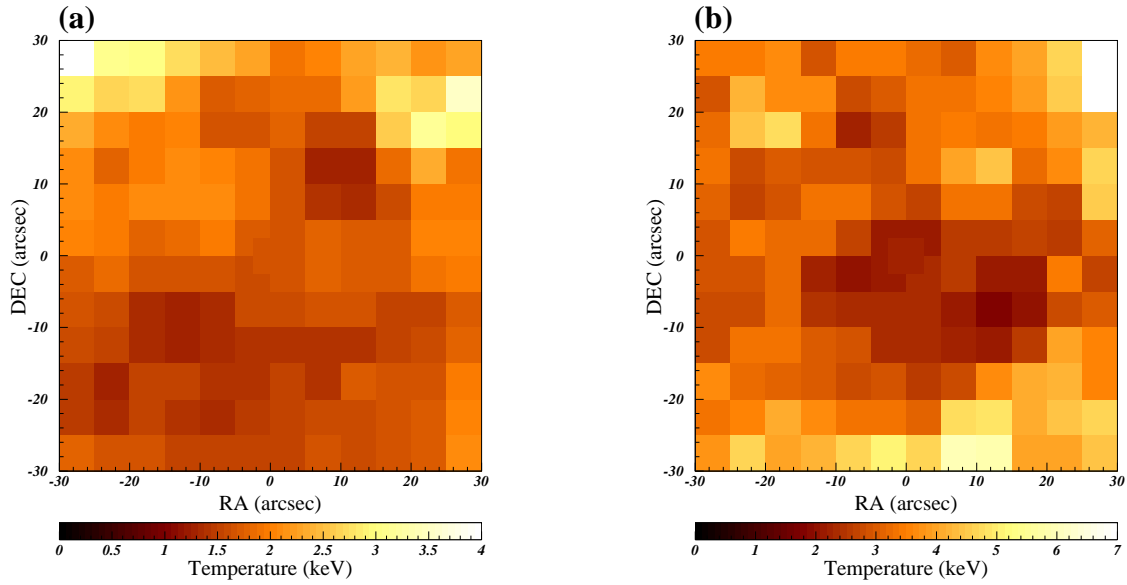


Fig. 5. Two-dimensional temperature maps of 2A 0335+096 (a) and A 2199 (b) in $60'' \times 60''$ around the cluster center. The darker regions correspond to lower temperature ones. Typical errors of temperature in each grid are 10% and 15% for 2A 0335+096 and A 2199, respectively.

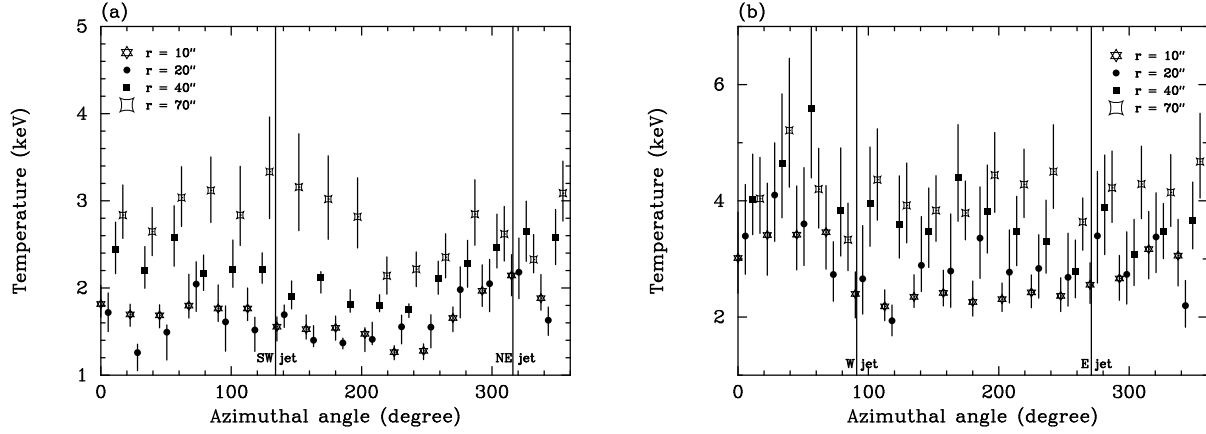


Fig. 6. Azimuthal temperature distributions of 2A 0335+096 (a) and A 2199 (b) on the four concentric annular regions, whose radii are $10''$, $20''$, $40''$, and $70''$ from the cluster center. The azimuthal angle is defined as 0° for the northern direction from the cluster center and increases clockwise.

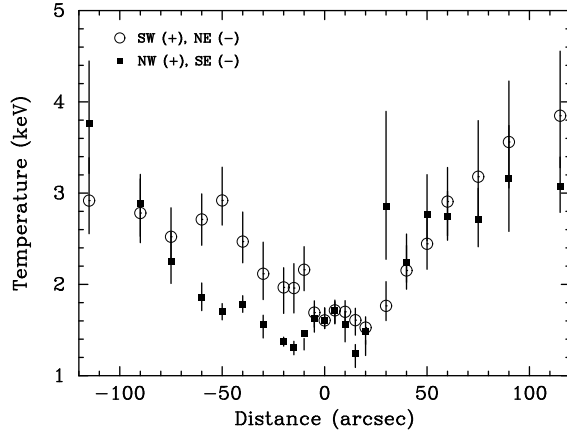


Fig. 7. Temperature distributions along the jet (open circles) and its perpendicular direction (filled squares) for 2A 0335+096. The horizontal axis is the distance from the cluster center in units of arcsec. Profiles along the SE (jet) and NE (perpendicular) directions are plotted in the positive region.